Integrated reservoir characterization of low resistivity thin beds using three-dimensional modeling for natural gas exploration

Lim Yen Jun & Lo Shyh Zung

Department of Geosciences
Universiti Teknologi PETRONAS, Seri Iskandar, Perak Darul Ridzuan
Corresponding author email address: limyenjun@gmail.com

Abstract: A natural gas reservoir was discovered at approximately 3 km (TVDSS) through first vertical wildcat. Four subsequent wildcats were drilled in deviated trajectory to assess hydrocarbon distribution with no success. Resistivity log response from hydrocarbon interval appeared as low value low contrast. Seismic acquired onshore with high degree of static variation resulted in low frequency, unable to delineate thin sand interval efficiently. Several hypotheses were formed to explain the failed discovery. First, geological structure is complex due to local tectonic deformities created faults that compartmentalized the reservoir. Second, hydrocarbon charge and migration pathway might be underestimated. Third, presence of high conductive mineral might affect the resistivity log acquisition. An integration of three-dimensional enhanced seismic horizon and fault interpretation, unsupervised machine learning in facies classification, petrophysical data conditioning, rock physics cross validation, and three-dimensional static modeling is used to provide clearer insight on the natural gas play.

Keywords: natural gas, low resistivity, thin bed

INTRODUCTION

Area of interest is located within West Taiwan Basin, a foreland basin developed by orogenic loading and flexure of rift-type continental margin, caused by oblique convergence between the Eurasian and Philippine Sea plates (Hirtzel, 1996). The study area is an extensional rifted Cenozoic foreland basin with Neogene petroleum system in extensive faulted region. This basin is regionally identified as purely sedimentary basin without influence from tectonic disturbance during deposition, controlled by sedimentation of shallow marine setting. It is believed the source of hydrocarbon was migrated from lower Miocene coal bed and deeper syn-rift deposits (Lin & Watts, 2002).

Success in hydrocarbon exploration in this region led to 2D seismic acquisition to study Yung Kuang subsurface structure which is located eastern side of Ba Zhang Xi structure. Yung Kuang structure is placed between two faulted structures, created a prominent two-way dip semi closure structural trap on (YK-1 Wildcat, n.d.). A major east-west Yung Kuang fault created an ideal horst and graben with largest throw measured around 1 km. Majority of younger formation in Yung Kuang structure were weathered due to uplifting event except a thick sequence of seal just above the target reservoir interval, Mu Shan. Previous geological research in nearby field showed that this reservoir interval has a homogeneous distribution of thickness at around 30 m (TVD) with an excellent net-to-gross ratio of 0.6 to 1.0. It is composed of fine to coarse quartz grain mixed with greyish shale making it a porous formation ideal for hydrocarbon accumulation.

Geochemistry research studies on lower flank of Mu Shan formation is a mature natural gas producing source rock. Hydrocarbon maturation starts during Pliocene to Pleistocene epoch, migrated from southeast to northwest into Yung Kuang structure reservoir formation. Bi Ling shale with deep marine facies acts as the seal, traps the accumulated hydrocarbon. The presence of validated source, reservoir, trap, seal, and migration pathway through geometry height and faults make this structure a valid and sound petroleum system.

Interpretation was performed on 2D seismic interpretation, it shows target reservoir has an accumulation area of 2.8 km^2, measured porosity from same formation at other well location at 17 %, water saturation is estimated at 30 %, and natural gas volume estimated at 60 %, with net pay sand interval of 15 m (TVD). Based on these parameters, it is calculated that Yung Kuang structure could be storing 18 B scf of natural gas. Exploration was carried out with a wildcat well drilled. Across all formations, mud log shows only Mu Shan formation with total gas measured at 45 to 62 units, with methane (CH_4) at 10277 ppm constitutes 70 % of natural gas types in the formation. Preliminary petrophysical interpretation using wireline logs obtained from wildcat indicates this formation has brine concentration of 14000 ppm, Rw at 0.17, Rt at around 20 ohm-m, ØD at 22 %, ØN at 15 %, and Sw at 38 %. These measurements indicate strong presence of natural gas in the formation with excellent producing capability.

PROBLEM STATEMENT

After the success of wildcat exploration that uncover potential of natural gas production, another exploration well was drilled southwest to previous wildcat to further access reservoir potential of this block. But wireline log returned a low resistivity reading led to high interpreted Sw, thus it was declared as a dry well (YK-2 Wildcat, n.d.). Additional three wells were drilled in different direction trajectories to access the extend of reservoir and understand subsurface geological variation but ended up as dry wells too. Two-dimensional seismic interpretation indicated strong signs of subsurface deformation due to extensional faulting, possibly compartmentalized the reservoir.

Source rock analysis and hydrocarbon geochemical analysis showed that the natural gas came from multiple sources, maybe from even deeper source rock where seismic cannot resolves successfully. It was also believed the source of hydrocarbon was not derived from Mu Shan formation itself, as prediction calculation made using James model thermal maturity showed that Ro of Mu Shan formation is 1.1 % but the Ro of Mu Shan formation sampled from first wildcat is at 0.6 %. It indicates deeper source of hydrocarbon, and with suitable migration pathway, there is a high possibility in discovering natural gas reservoir nearby.

Interpretation made from mud log and gamma ray response showed Mu Shan formation is about 15 to 20 m (TVD) thick with interbedded sand shale sequence. The tuning frequency of seismic wavelength is much larger than formation thickness, affects the delineation of formation top and bottom from adjacent formations. Another challenge comes from low resistivity response from detected formation with low contrast compared to adjacent water leg, which might be caused by high concentration of pyrite mineral in the formation. Moreover, presence of numerous minor faults and complex tectonic events caused some problems towards onshore seismic processing with datum static irregularity.

This research is designed to characterize and identify the underlying issue in this reservoir, to understand subsurface structures and compartmentalization through qualitative seismic interpretation and to carry out integrated reservoir characterization with three-dimensional modeling on target Yung Kuang structure.

DATA AVAILABILITY AND METHODOLOGY

Approximately 10 km^2 of an onshore area was selected for 3D seismic acquisition. Seismic data consists of the raw shots, static datum, processed pre-stack CMP gathers and seismic stack. A necessary step to generate accurate coordinate referencing system was then required because the acquisition did not use conventional coordinate system in software's library. Wildcat wells' LAS format files were then collected, inclusive of all available wireline logs data. This includes but not limited to: gamma ray, spectral gamma ray, corrected gamma ray. Caliper, bit size, spontaneous potential, compressional sonic, enhanced resolution induction deep resistivity, enhanced resolution induction medium resistivity, neutron porosity, sonic porosity, and density. Well deviation trajectories and lithology information from mud log are obtained as well. The drill stem test result for the successful wildcat was analyzed for hydrocarbon occurring information.

A. Log quality check and conditioning

Prior to petrophysical calculation and interpretation, necessary well log editing and conditioning is important in ensuring the integrity of multiple well logs (Asquith & Krygowski, 2004). In this dataset, gamma ray logs are corrected to eliminate the effects of radioactive mineral, Uranium. It formed because of chemical weathering but it is unstable compared to potassium and thorium and usually trapped in sediments which affects the reading of gamma ray values (Schön, 2015). Thus, the correction enhances the separability of sand and shale more effectively in sediments dominant environment. Bulk Density and Compressional Sonic are crucial for synthetic seismogram; hence QC and correction are mandatory to reduce errors of uncertainty during computation. Compressional sonic log is the most important log for time-depth relationship, thus it shall be carefully corrected for noise spikes, washouts, and abnormal

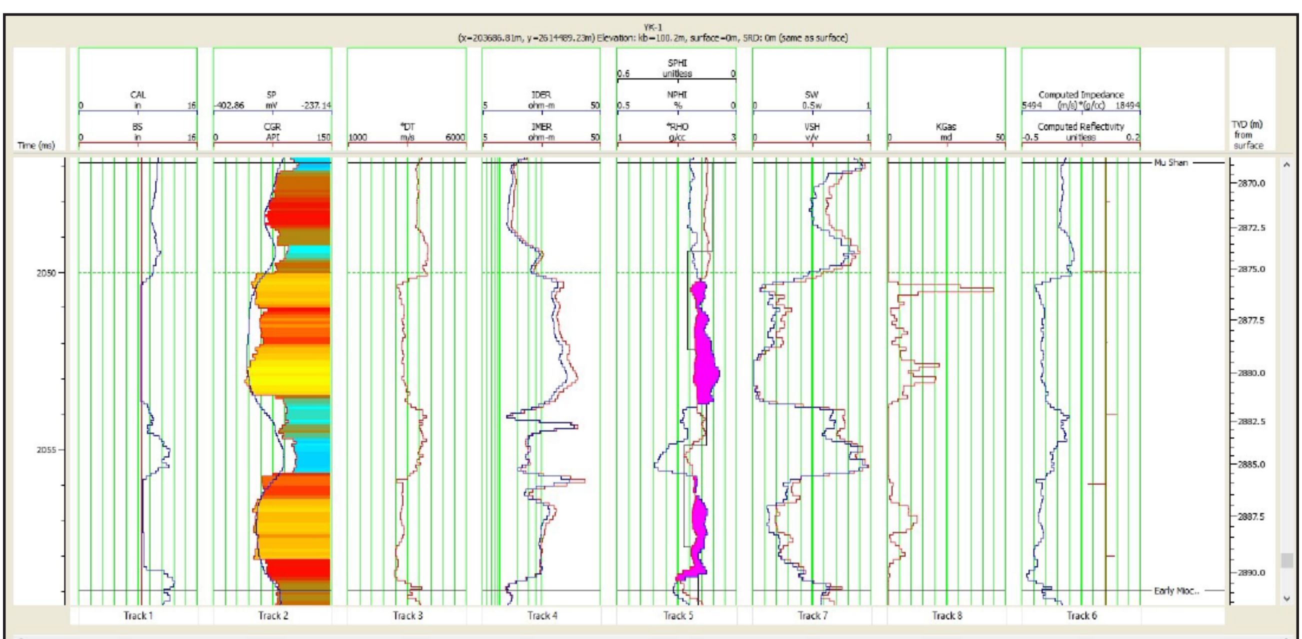

Figure 1: Wireline logs display template at target reservoir interval.

values range. Since check shot is not acquired, preliminary synthetic seismogram is generated to validate the data validity of processed sonic log.

The key to a good synthetic seismogram is scaling the well data to the seismic bandwidth for a better relationship between well and seismic. This can be achieved through effective medium theory where averaging methods represent thin isotropic layers and its elastic properties while maintain dominant geological signature (Avseth *et al*., 2005). Backus averaging method is chosen in this research and original well log will be blocked according to input logs: compressional wave velocity, shear wave velocity, and density.

B. Facies classification and well correlation

The incorporation of multi-well logs and lithological report made unsupervised machine learning facies classification possible. Lithological logs such as gamma ray, porosity, density, sonic are used to generate initial principal component analysis model (Hall, 2016). The facies classification is then filtered to be sandstone and shale sequence as the research focuses on sand reservoir interval. These created facies log for each well indicating sand and shale lithological layers. From the mud log interpretation report, well tops are marked according to the formation name and its associated measured depth. Well correlation is then carried out for all wells to study the lateral continuity of lithological occurrence. After well correlation, the relationship between different log signatures at different formations can be compared to the geological lateral continuation. It is especially important for a highly faulted, compartmentalized and high variation in fluid content in this research.

C. Seismic well tie

The wavelet is created through deterministic method, known as Extended Roy White algorithm. The wavelet generated through the computation using cross correlation of the reflectivity and the seismic trace in frequency domain, autocorrelation of reflectivity and white noise factor. This method can effectively determine optimal time shift between well log reflectivity and seismic amplitude, the dominant phase of wavelet and provides statistical index in determine the quality of well tie. Integrated seismic well tie is carried out by carrying out sonic calibration and synthetic generation in one single process, every edit is updated real time to observe immediate effects of altered parameters to allow fast parameter optimization deployment and quality control of statistical wavelet and calibrated sonic. Time depth relationship is generated through conditioned sonic log and velocity information computed. Acoustic impedance and reflection coefficients are computed through corrected sonic and density log. Synthetic seismogram is then generated by convolving wavelet and reflection coefficients. The result allows understanding of seismic response of lithologies and fluids at well location, the phase characteristics and tying well tops to seismic for accurate seismic horizon interpretation later.

D. Seismic volume attributes and direct hydrocarbon indicator (DHI)

The seismic data must be carefully loaded according to correct trace locations and coordinate information system to visualize it at real world coordinates. Original SEG-Y 3D seismic cube is too large for the capability of software handling and rendering. The seismic cube is realized into software's preferred bricked format with amplitude values rescanned and resolution lowered (but not affecting data quality). Random line can be generated from any azimuth and dip to visualize the seismic section along the line, this is made possible from a 3D seismic cube.

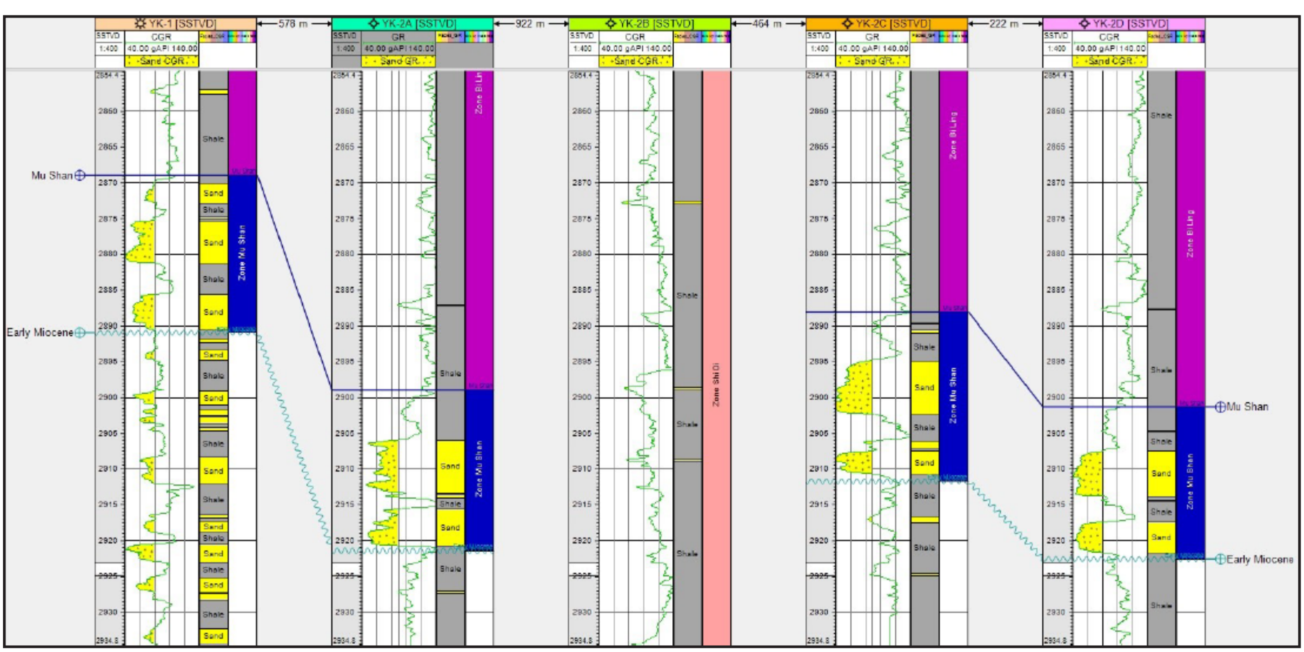

Figure 2: Facies classification and well correlation.

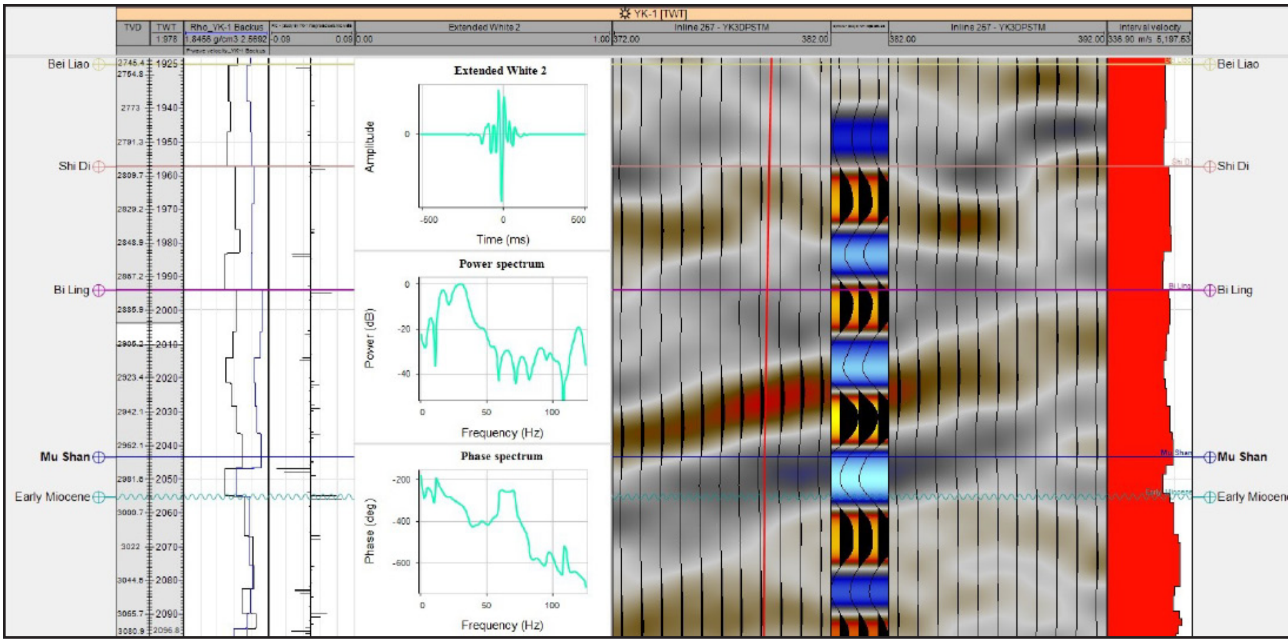

Figure 3: Integrated seismic well tie using Extended Roy White deterministic wavelet.

Volume attribute computation allows us to generate new seismic volume that is optimized for different interpretation and visualization purposes due to different algorithms emphasizing different aspects of seismic information (Chopra & Marfurt, 2007). Out of many volume attributes available, only few volume attributes are proven effective in this research. Structural smoothing attribute makes use of principal component dip and azimuth to determine local structure then uses Gaussian smoothing to increase the continuity of the seismic reflectors. This attribute is enhanced with edge detection to preserve discontinuity information. It is also useful to illuminate fluid contacts that is horizontal in nature, while improves the process of horizon interpretation later. Variance attribute is effective in recognizing fault edges by estimating local variance in the seismic signal, added with dip correction and plane confidence, it can be used to accentuating structural features (Randen *et al*., 2000).

DHI study is based on first pass seismic interpretation at well location. Since shallow unconsolidated hydrocarbon bearing sandstone reservoir historically having a pronounce bright spot feature and flat spot fluid contact in the reservoir, this signature is the first to be scanned and observed (Simm & Bacon, 2014). Based on the quick rock physics study on the lithological sequence and associated predicted seismic response, any anomaly differs from expected non-hydrocarbon scenario is observed (Herron, 2011). For example, push down effect of velocity sag effect for gas pockets and "eyeball" anomaly for high porosity zone. Sweetness volume attribute can be used to highlight bright spots or identify changes in overall energy signatures. This attribute made use of envelope and instantaneous frequency. But the reservoir in this research is thin bed which is affected by seismic tuning thickness issue, many attributes couldn't produce effective results (Zeng & Marfurt, 2015).

E. Fault and horizon interpretation

It was hypothesized that the reservoir is highly compartmentalized, hence a noble fault interpretation workflow is required to illuminate sub-seismic fault through effective method. The poor signal to noise ratio, presence of different noises, and limited processed and migrated seismic volume proved difficult for straight forward fault interpretation. Ant Tracking workflow is adapted for fault extraction through seismic conditioning, fault preserving volume attributes, stereo net geomechanics stress isolation and prediction, and ant track volume which improves fault attributes by suppressing noise and other non-faulting events in seismic (Klem-Musatov *et al*., 2008). Signal tracker finds optimal connectivity for fault features by estimate orientation of identified local maximum. This method can be used to extract major regional faults or subtle fault zones in the seismic data according to preference. The extracted faults are then filtered through orientation filtering to removes abnormal faults, and the remaining faults are then analyzed and merged accordingly. This workflow produced a reliable fault model for the highly compartmentalized reservoir in the research.

The geological structure bounded by survey is highly folded and faulted with highest fault throw of 1 KM. The strike of major geological layers is determined before horizon interpretation is carried out. This is done by visualizing different seismic section across seismic lines at different azimuth. Once the strike and dip direction of the seismic is determined, seeded 3D auto tracking is chosen for horizon interpretation. Seismic data conditioning and enhancement were carried out numerous times to ensure best input for efficient auto tracking (Bucknill, 2006). The interpreted horizons are the top of sand and base and top of underlying unconformity of the reservoir interval. Auto tracking prioritize picks of higher extrema and picks with shortest expansion path to ensure best quality seed expansion in automated horizon auto tracking. Necessary signal features such as phase, polarity, wavelet tracking etc. are tweaked to give optimum horizon interpretation.

F. Structural framework and 3D modeling

The goal of geophysical research is using acquired numerical data in creating a subsurface model that helps us evaluate the geological properties of subsurface, where it is invisible for visualization. With the availability of 3D horizon interpretation and structural interpretation, fault interpretation, and geological layers information, we can generate an accurate structural framework. This framework represents the geological structures and will be used for volume calculations, uncertainty analysis, upscaling and preferably well design. The relationship between different fault planes and their interactions with geological is honored compared to traditional corner point gridding. Validated well tops are used for guiding horizon modeling properly, adjusted further with isochron properties of different wells. Once a proper structural framework is created, the zones inside the framework is used for different calculations on gross rock volume or predicted fluid volume. To facilitate simulation study in the future, a traditional corner point gridding can be generated using existing framework. Pragmatic grids with predefined size of grid cells are useful for incorporating upscaled well log and reduce the resources needed to simulate a dynamic model.

Facies modeling is the next crucial objective of creating a valid subsurface model. Through distributing discrete data, different methods of stochastic and deterministic can be used to model the facies distribution in the reservoir (Dubrule, 2003). The integration of upscaled facies well log generated through machine learning classification previously, modeling parameters and modeling mechanism, the population of sandstone facies and shale facies in the reservoir can be visualized in 3D. In this research, sequential indicator simulation which is only used for discrete data is used for distributing the facies property stochastically in the model. This method uses predefined frequency distribution of upscaled data points and random seeding to propagate facies property, particularly useful for uncertain facies distribution. Petrophysical modeling interpolates porosity data from petrophysics datasets interpreted through well log petrophysical interpretation. As the well control is not sufficient, sequential Gaussian simulation (stochastic) is used. It honors well data, input distributions and random seeds to represents propagation of petrophysical data.

RESULTS AND DISCUSSION

The identified reservoir interval is between well tops Mu Shan and Early Miocene Unconformity. In Figure 1 the first track showing Caliper log has a similar diameter with 8 inches bit size, indicating no washout or significant caving on sand facies at reservoir interval. Second track of Corrected Gamma Ray log showing lower number of counts on sand facies and its trend is validated by Spontaneous Potential log indicating confirmation of sandstone lithology. Third track of Compressional slowness showing decrease in compressional wave velocity on sand facies, due to porous sandstone formation and presence of natural gas. Fourth track shows abnormally low resistivity values (around 15 to 25 ohm-m) despite contrast in much smaller scale indicates high electrical conductivity within reservoir interval that needs attention. Resistivity log's scale is reduced to 2.5% of recommended display scale. Following industrial convention, density-neutron log is displayed in defined scale and polarity. A crossover between porosity logs and density log confirmed the presence of porous sandstone formation, the butterfly crossing event is usually associated to hydrocarbon bearing zone. By using Dual Water saturation model, average water saturation of 40% (lower than 10% on sand facies) is calculated, net to gross ratio at 70%, associated with low shale volume on sand facies. The total thickness of this interval in this well is 22 m. Drill stem test was carried out showing the reservoir has 62 units of Total Gas Unit, consists of 78% methane natural gas, and production rate at 125 000 scm per day. There was no attempt in interpreting depositional environment through gamma ray log shape and features as the methodology is oversimplified and non-reliable (Rider, 1990).

Facies classification of major sand and shale facies is generated through machine learning incorporating multiple wireline logs input as mentioned earlier. In Figure 2 the facies are compared with zone indexes to ensure good tie between geological layers and facies estimation. Well correlation is then conducted to link wells together by geological means and found significant height variation despite these deviated wells are neighboring to each other. One well did not encounter reservoir interval even at deeper location. As the formation was deposited in shallow marine environment, it is fluvial deltaic tidal dominated sedimentation (Slatt, 2013). Hence, it is thin and interbedded.

Although without check shot information, the time depth relationship is accurate with accurate reflectivity response at seismic domain as shown in Figure 3. Underlying issue of seismic processing difficulties led to reflection coefficient inconsistency between well logs and seismic data, but deterministic Extended Roy White wavelet can convolve with reflection series at accurate frequency and phase. Strong visual correlation is observed at Mu Shan and Early Miocene well tops. Thin bed nature caused top and bottom separation due to seismic tuning thickness. Correct time depth relationship is crucial for horizon picking.

In Figure 4 (top) easily observed the presence of low frequency noise and poor seismic reflection lateral continuity. Onshore seismic acquisition with challenging static profile often led to poorer image compared to offshore. In this figure, an inline is selected for display as it coincides with local dip showing two-way semi dip closure anticlinal trap structure. Reservoir top is represented by bright negative polarity seismic reflection (blue) underlaid by burdening shale formation (red). Bright reflection indicates increased reflection coefficient, the results of increased impedance

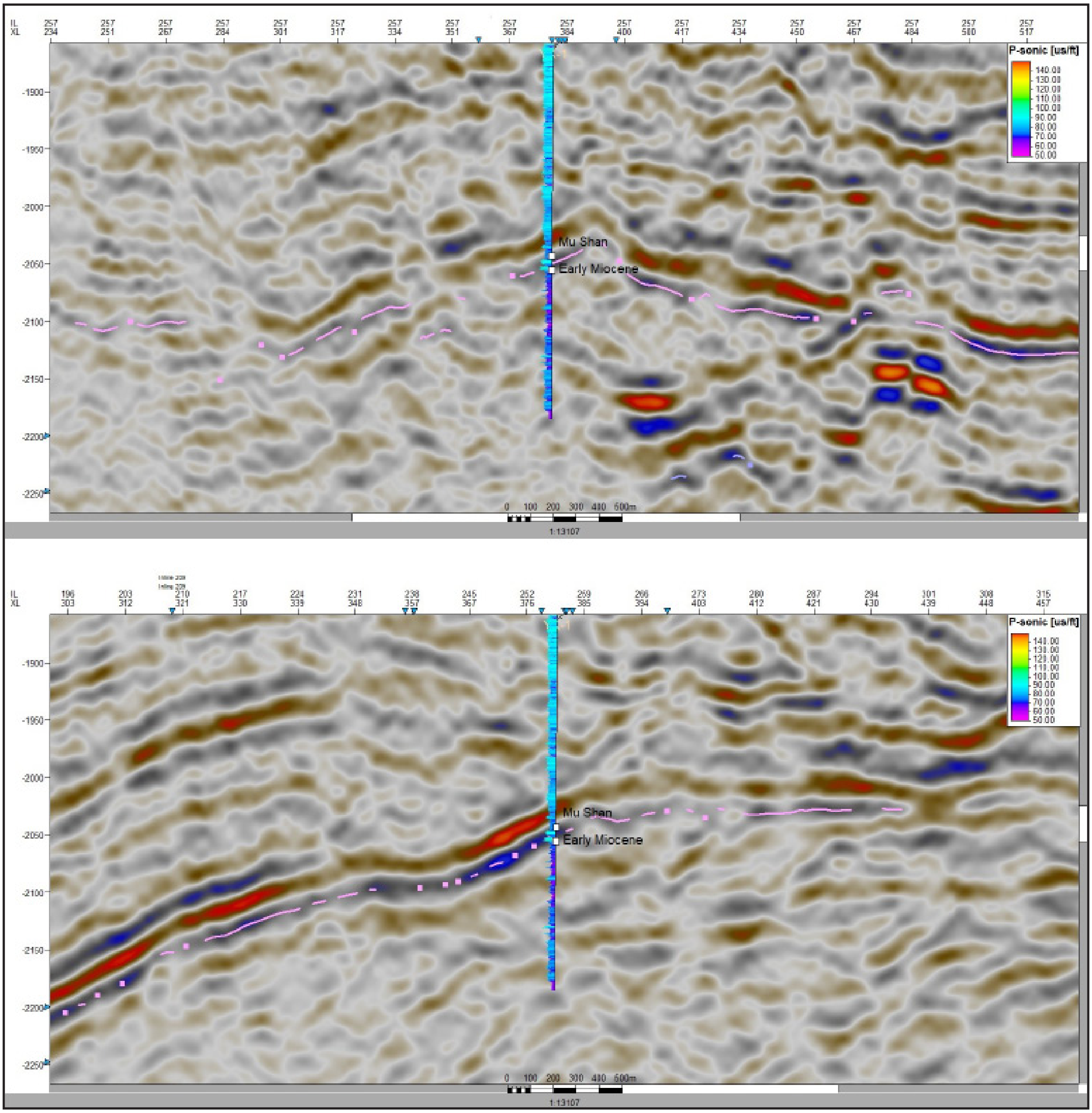

Figure 4: Seismic inline (top) and strike line (bottom) showing reservoir target and seismic response.

contrast between overburdening formation and target formation due to significant decrease in velocity and density values. Unfortunately, pre-stack CMP gather analysis indicates a poor seismic reflector event continuity through offsets, might be the reason why the reservoir top is dimmer than it shall be. In this seismic stack, seismic reflector below the reservoir experienced pushdown effect possibly due to natural gas accumulation. A sudden abrupt change in velocity profile causes migration of seismic reflectors ineffective to position them at accurate position, led to increase in apparent travel time. Conventional "eyeball" effect can be seen where strong fluid contact response within the reservoir formation causes a reflection separation in homogenous reservoir layer. Another seismic line shown in Figure 4 (bottom) represents the major regional strike direction is displayed. Similar result from seismic analysis and DHI study can be obtained. Interesting observation is the sudden disruption in seismic reflection strength and continuity at target reservoir anticlinal trap, which is explained through poor seismic reflector continuity across offset traces in pre-stack CMP gathers.

Structural smoothing provides a seismic volume with better seismic reflection continuation and magnitude while preserving edge properties for discontinuities. The amplitude was rescanned for a better visualization and auto tracking process. Sweetness attribute shows strong bright spot outside of well control at north-west region. Variance attribute enhances discontinuity illumination for stratigraphic interpretation, indicating multiple major faults and numerous minor faults with obvious strike and dip of geological structure. Figure 5 shows all types of seismic volume attributes used in this research. The geobodies in this figure were generated using interpreted horizons as guide with defined thickness and guiding algorithms.

Figure 6 shows full scale facies model and effective porosity model generated through structural framework followed by pillar gridding. The model is converted in depth domain using single well velocity. With the final model created, it is easy to calculate or visualize the distribution of both discrete data and continuous data propagation. Figure 6 is the high density, structure focused, time domain model with better fault model. Although it took much more effort to generate such model under the influence of data limitation, but it gives a clearer understanding on the reasons why some wells failed to produce. There are multiple faults presence in such small structure causing different underlying problem, such as non-sealing fault plane allowing hydrocarbon seepage, compartmentalization causing ineffective hydrocarbon accumulation, and possible different routes of hydrocarbon migration pathway instead to the highest anticlinal structure (Jenyon, 1990).

CONCLUSION

Throughout intensive integrated reservoir characterization workflow, it is undeniable that Mu Shan formation in Yung Kuang subsurface structure has a great potential accumulating significantly large amount of natural gas. However, the pyrite minerals found in the formation could pose problem for reevaluation of existing wildcat as it induced low resistivity issue. Thin Mu Shan formation with high degree of lateral height variation introduced difficulties in seismic imaging and prospect identification. Complex tectonic history involving extensional faulting and inversion created numerous isolated compartments in the reservoir. To overcome these challenges, special logging tool such as Nuclear Magnetic Resonance is recommended to identifying presence of hydrocarbon. More drill stem tests should be carried out in previous failed wildcats as low resistivity might not related to absence of hydrocarbon but influences of pyrite minerals on conductivity.

ACKNOWLEDGEMENT

I thank Geological Society of Malaysia for providing the opportunity to showcase my research and share it with many brilliant minds. I would also like to show my gratitude to my colleagues in Department of Geosciences,

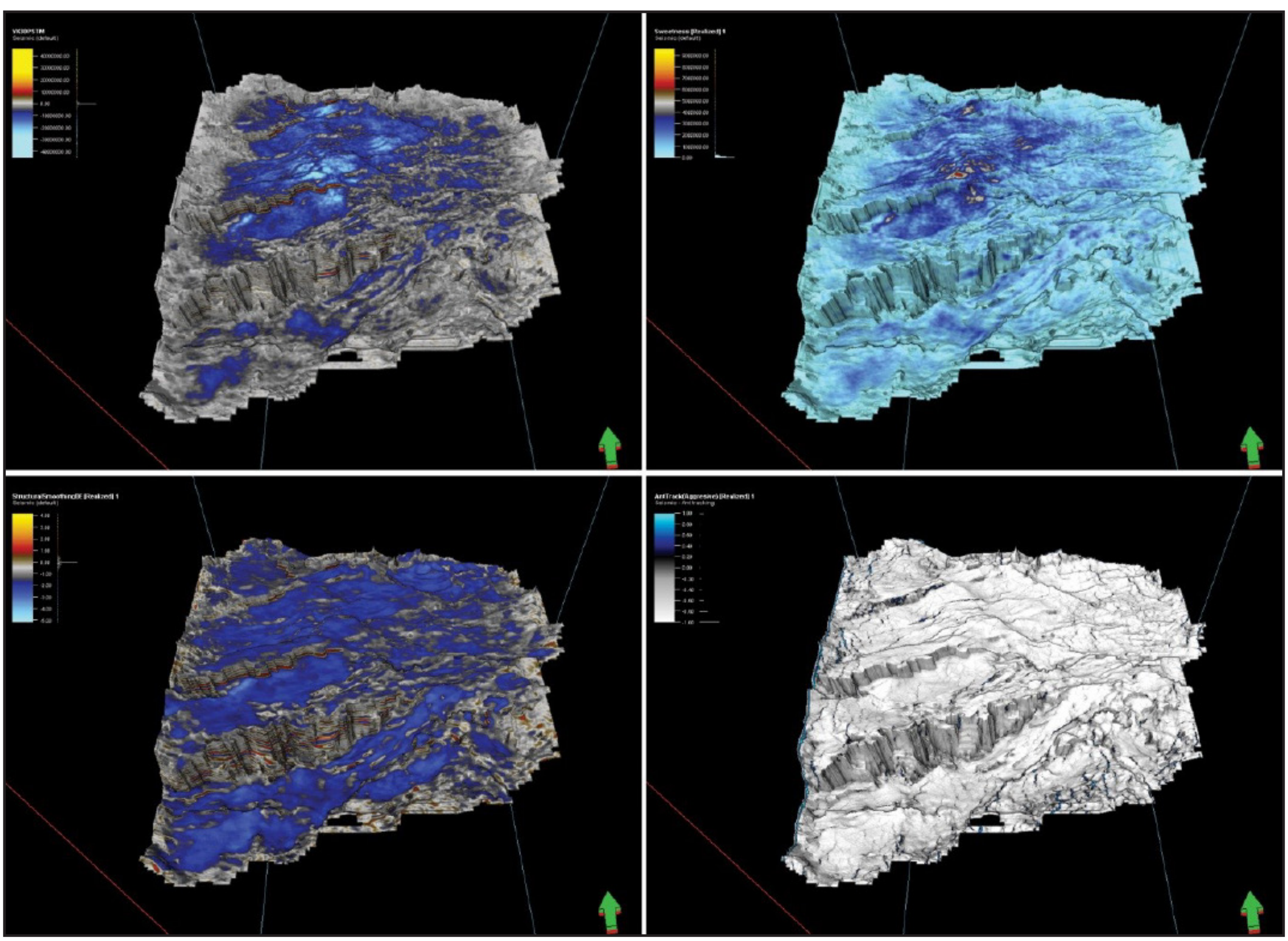

Figure 5: Geobody probe visualization of different seismic volume attributes. Upper left: Original Seismic, Upper right: Sweetness, Lower left: Structural Smoothing, Lower right: Ant Tracking).

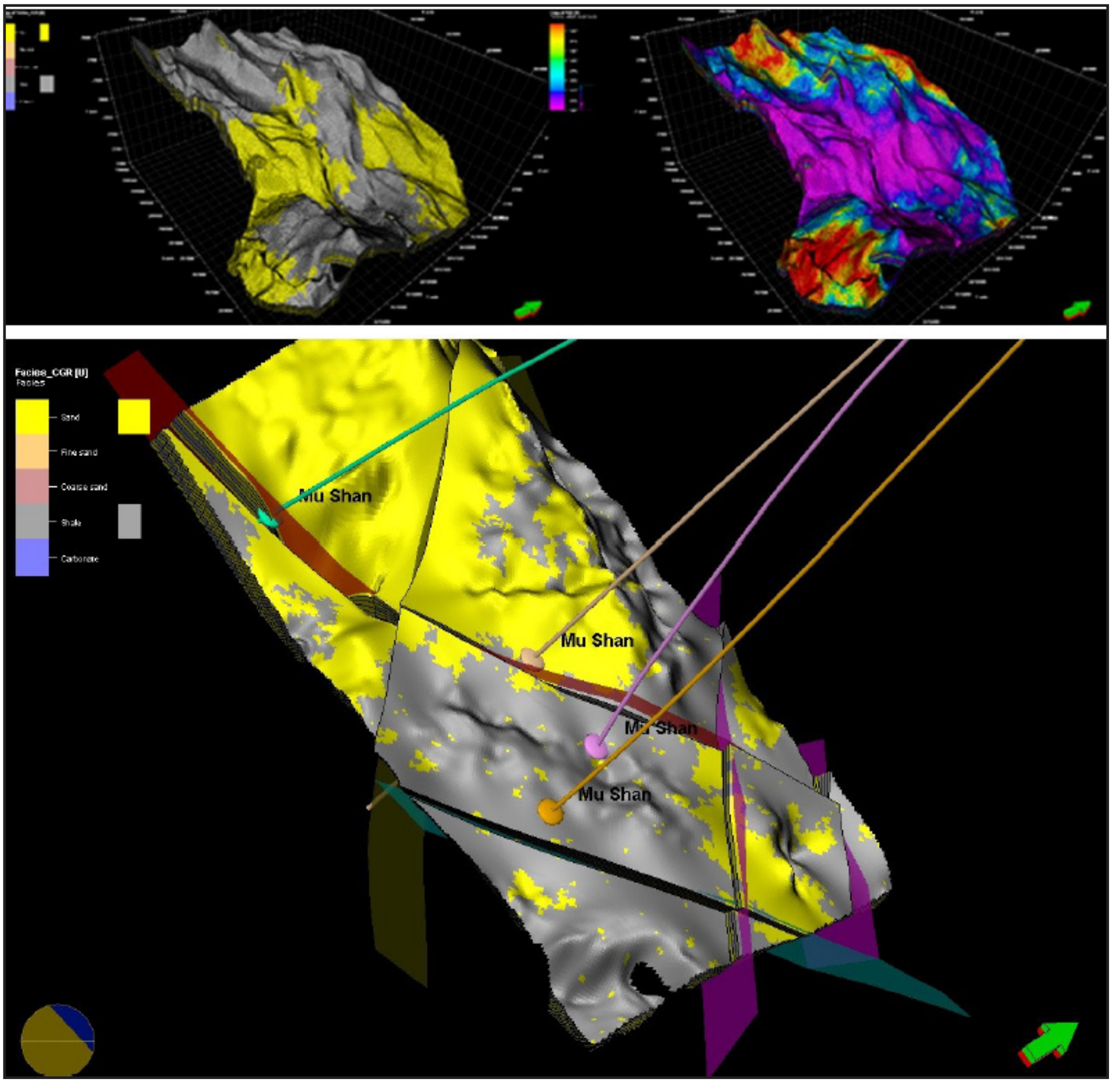

Figure 6: 3D facies model (upper left), effective porosity model (upper right), and high density target area facies model (bottom).

Universiti Teknologi Petronas who provided insights and expertise that made this research a success.

REFERENCES

Asquith, G. & Krygowski, D., 2004. Basic Well Log Analysis (2nd ed.). Oklahoma: American Association of Petroleum Geologists. Retrieved from www.aapg.org.

Avseth, P., Mukerji, T. & Mavko, G., 2005. Quantitative Seismic Interpretation Applying Rock Physics Tools to Reduce Interpretation Risk. Cambridge University Press, Cambridge. 359 p.

Bucknill, M.J., 2006. Volume Interpretation Workflows; Practical considerations, Advances in Automation and Efficiency. Proceedings of the 8th SEGJ International Symposium. Doi: 10.1190/segj082006-001.115.

Chopra, S. & Marfurt, K.J., 2007. Seismic Attributes for Prospect Identification and Reservoir Characterization. Oklahoma: Society of Exploration Geophysicists. Retrieved from http://library.seg.org/.

Dubrule, O., 2003. Geostatistics for seismic data integration in earth models. Distinguished Instructor Series, No.6., Tulsa, USA, Sponsored by the Society of Exploration Geophysicists and the European Association of Geoscientists & Engineers.

Hall, B., 2016. Facies classification using machine learning. The Leading Edge, (October), 906–909.

Herron, D.A., 2011. First Steps in Seismic Interpretation. (Rebecca B. Latimer, Ed.), Geophysical Monograph Series, No. 16, by Society of Exploration Geophysicists, Tulsa, Oklahama.

Hirtzel, J.O., 1996. Evolution of a forearc basin in arc-continent collision, offshore Taiwan. Retrieved from http://scholarworks.sjsu.edu/etd_theses.

Jenyon, M.K., 1990. Oil and Gas Traps Aspects of their Seismostratigraphy, Morphology, and Development. John Wiley & Sons, Chichester, New York, Brisbane, Toronto, Singapore. 398 p.

Klem-Musatov, K., Aizenberg, A.M., Pajchel, J. & Helle, H.B., 2008. Edge and Tip Diffractions Theory and Applications in Seismic Prospecting. By Society of Exploration Geophysicists, Oklahama. Retrieved from http://library.seg.org/.

Lin, A.T. & Watts, A.B., 2002. Origin of the West Taiwan basin by orogenic loading and flexure of a rifted continental margin. J. Geophys. Res., 107(B910). https://doi.org/10.1029/2001JB000669.

Randen, T., Monsen, E., Signer, C., Abrahamsen, A., Hansen, J.O., Saeter, T., Schlaf, J. & Sonneland, L., 2000. Three-dimensional texture attributes for seismic data analysis: SEG International Meeting.

Rider, M.H., 1990. Gamma-ray log shape used as a facies indicator:

critical analysis of an oversimplified methodology. Geological Society, London, Special Publications, 48(1), 27–37. https://doi.org/10.1144/GSL.SP.1990.048.01.04.
Schön, J.H., 2015. Physical properties of rocks: Fundamentals and principles of petrophysics (Vol. 65). Elsevier, 121-133.
Simm, R. & Bacon, M., 2014. Seismic Amplitude An Interpreter's Handbook. Cambridge University Press, New York. 271 p.
Slatt, R.M., 2013. Stratigraphic Reservoir Characterization for Petroleum Geologists, Geophysicists, and Engineers. Elsevier, Amsterdam. 492 p.
YK-1 Wildcat. (n.d.).
YK-2 Wildcat. (n.d.).
Zeng, H. & Marfurt, K.J., 2015. Recent progress in analysis of seismically thin beds. Interpretation, (August). https://doi.org/10.1190/INT-2014-0232.1.

Manuscript received 2 October 2017
Revised manuscript received 16 April 2018
Manuscript accepted 18 April 2018